European Radiology (2019) 29:1365–1374
https://doi.org/10.1007/s00330-018-5691-9

HEAD AND NECK

Ex vivo orbital volumetry using stereology and CT imaging: A comparison with manual planimetry

Georgios Bontzos[1] · Michael Mazonakis[2] · Efrosini Papadaki[3] · Thomas G. Maris[2] · Styliani Blazaki[1] · Eleni E. Drakonaki[4] · Efstathios T. Detorakis[1]

Received: 18 April 2018 / Revised: 20 June 2018 / Accepted: 31 July 2018 / Published online: 22 August 2018

Abstract

Objectives To evaluate the applicability of stereology and planimetry in orbital volume measurements using computed tomography (CT) and to compare the results between the two measurements.

Methods Experimental study using sheep craniums for CT imaging. Water filling measurements were performed, as the validation technique. Quantification techniques were also evaluated in five human subjects. To examine the proportion of agreement among measurements, we tested intra- and inter-observer agreement.

Results For stereology customization, a 1/8 systematic sampling scheme was considered as optimal; this resulted in a low coefficient of error (2.59 %) and low measurement time (1.9 mins). In sheep craniums, mean volume measured by water displacement, planimetry and stereology was 17.81 ± 0.59 cm^3, 17.87 ± 0.68 cm^3 and 17.54 ± 0.49 cm^3, respectively. Total volumes, obtained by stereology, were highly correlated with the water-filling method (r=0.893; $p = 0.001$) and a paired t-test showed significant difference between methods (t=3.047; $p = 0.014$). Planimetry results displayed a high correlation with the water-filling method (r=0.957; $p \approx 0.001$) but no statistically significant difference was found ($p = 0.154$). Mean difference using planimetry and stereology was 0.332 ± 0.322 cm^3. In human subjects, using stereology, the estimated volume ranged between 18.57 cm^3 and 19.27 cm^3, and the mean orbital volume was 19.05 ± 0.50 cm^3 with CE=3.75 ± 0.16 %. Mean measure time was 2.1 ± 0.1 mins.

Conclusions Stereological measurements were superior to manual planimetry in terms of user effort and time spent. Stereology sampling of 1/8 was successfully applied in human subjects and yielded a strong correlation with manual planimetry.

Key Points

- *Stereology can be applied to measure the orbital volume using computed tomography.*
- *Stereological measurements display high correlation with gold standard planimetry and combine low coefficient of error (2.59%) with low measurement time (1.9 min).*
- *Stereology is superior in terms of user effort and time spent.*

Keywords Orbit · Eye · Skull · Anatomy

✉ Georgios Bontzos
gbontzos@hotmail.gr

[1] Department of Ophthalmology, University Hospital of Heraklion, 71110, Stavrakia, Heraklion, Crete, Greece

[2] Department of Medical Physics, University of Crete, Heraklion, Greece

[3] Department of Radiology, University Hospital of Heraklion, Heraklion, Greece

[4] Independent Imaging Services, Heraklion, Crete, Greece

Abbreviations

CE	Coefficient of error
CT	Computed tomography
ICC	Intraclass correlation coefficient
MRI	Magnetic resonance imaging
SD	Standard deviation

Introduction

Orbital volume measurements serve as an invaluable tool for surgeons and clinicians. Quantitative determination of orbital volume has a crucial role in pre- and postoperative

management of maxillofacial fractures, such as blowout fractures [1], and in developmental osseous abnormalities [2]. In addition, careful calculations allow the design of customized patient implants to correct volume deficits after orbital decompression or for correcting exophthalmos as seen in Graves' disease [3]. In fact, a small change in volume can cause axial movement of the eye [4.] Therefore, precise measurements are needed. The demand is becoming more prevalent in the modern era of 3D-printing where orbital reconstruction has become even more accurate [5]. However, there is little consensus on a standardized orbital volume technique. Volume changes are often visually estimated based on the physician's personal experience without direct measurements.

Computed tomography (CT) is still the most popular established method for evaluation of craniofacial injuries, as it can be used to delineate osseous structures and soft tissue. Over the past decades, several studies have attempted to manually quantify the orbital volume and validate the respective measurements [6–10]. However, manual segmentation has numerous drawbacks. A single accurate measurement of the desired area may require several hours, while the results are inter-observer sensitive and can vary up to 15% between experts [11]. The eye socket is not simply cone-shaped, but has complex concavities and convexities and different volumes between individuals. Current CT technology has become significantly more advanced, offering higher resolution images and thinner slices. Despite the technological improvements, determination of the orbital volume remains challenging. The orbital median wall and floor are very thin structures and their boundaries are not well defined. This can be partially explained by the partial volume effect [12], where admixing signals within a voxel result in rough delineation of individual tissues. Awareness of the limitations in orbital volume segmentation is crucial to differentiate between true measurements and calculation errors. Significant errors may arise either from the imaging protocol or the post-processing analysis and lead to false computed volumes.

A method for quantification of the orbital volume needs to be clinically orientated. Therefore, its applicability depends on how quick, accurate and versatile it is [13]. Current approaches include two main methods: planimetry and stereology. Planimetry is considered the most prevalent technique and is based on the summation of manually delineated areas obtained from a series of CT slices. Stereology in based on the statistical point-counting process, and has been tested to measure the orbital volume [14, 15]. Sample point-counting methodology is based on the Cavalieri principle, which states that the volume of an object can be calculated using its two-dimensional parallel sections, separated by a certain distance [16, 17]. For instance, volume measurements can be obtained from an organ of interest after cutting it from end-to-end starting at a random position and continuing on a set of equally-spaced parallel section planes [18, 19]. To the best of our knowledge, no attempts have been made to evaluate both planimetry and stereology and investigate their overall performance for the orbital cavity at the same time.

There were two aims in this study: (i) to provide a comprehensive analysis of the validity, reliability and repeatability of orbital volume measurements by application of stereology and planimetry in CT image datasets obtained from sheep cranium. For validation, results are compared with the water-filling method, based on Archimedes' principle [14]. (ii) To compare the stereological results with those obtained with manual planimetry.

Furthermore, we examined the validity of the tested quantification techniques in patients referred to the Department of Radiology who were disease-free in the orbital area.

Materials and methods

This was an experimental animal study based on the imaging of the sheep cranium. Five sheep heads (total of 10 orbits) were provided by the animal house of the University of Crete, Faculty of Medicine. Sheep were sacrificed on the same day as imaging and water-filling experiments. To examine the applicability of our tested methods we also used the described imaging and quantification techniques in five human subjects who were referred to the Department of Radiology of the University Hospital of Heraklion and were diagnosed as disease-free in the orbits and the periorbital area. All the experimental animal procedures followed the ARVO Statement for the Use of Animals in Ophthalmic and Vision Research and the institutional guidelines. The study was approved by local ethics committee and adhered to the tenets of the Declaration of Helsinki. The purpose of this study was explained to all participants, who gave signed written consent.

Image acquisition

The imaging protocol consisted of CT scans using the standard orbital protocol using a 16-detector row CT system (Somatom Sensation 16, Siemens, Erlangen, Germany). The reconstructed slice width was always 0.625 mm and the mean pixel dimensions were 0.301 × 0.301 mm. The same imaging protocol was applied for the sheep craniums and for human subjects.

Exenteration of the eye socket/surgical technique

After the image datasets were obtained, each orbit was carefully dissected to remove all soft tissue from the orbital cavity

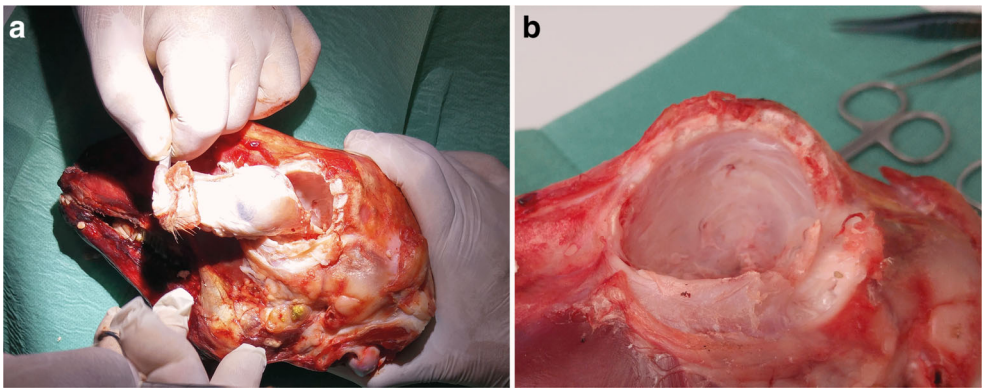

Fig. 1 **a** Enucleation procedure of the soft tissue from the orbital cavity. The entire orbital contents were removed *en bloc* down to the optic canal. **b** The orbital socket was immobilized in a perfectly horizontal direction. The orbital cavity was filled by water to determine the orbital volume

following the standard enucleation procedures (Fig. 1a). The entire orbital contents were removed *en bloc* down to the optic canal. The soft tissue, the extraocular muscles and the orbital fat were removed. The globe and the optic nerve were isolated separately. The optic nerve was separated from its canal part at the optic foramen. The jugular and oval foramen were carefully sealed using clay.

Water-filling method

The anterior boundary of the orbit was defined as the line that connects the two end-points of the front medial and lateral wall. The skull was afterwards immobilized in a way that the anterior boundary was perfectly horizontal. The remaining orbital socket (Fig. 1b) was filled with water to determine the orbital volume by measuring the quantity of the required water. This method relies upon the Archimedean principle of fluid displacement, which states that an object displaces its own volume when immersed in water.

Planimetry technique

DICOM images were analyzed using the open-source imaging processing software 3D Slicer v.4.6.0 for image segmentation, by applying manual 3D volume rendering. The orbit boundaries were manually delineated in axial slices (Fig. 2a) by two separate, experienced researchers to test inter-observer reliability. The posterior boundary of the orbit was defined as the crossing line between the median and lateral walls of the cavity around the optic foramen. The volume (V) of the segmented orbital cavity (Fig. 2b) was calculated by Eq. 1:

$$V = \sum_{i}^{m} (Ta_i)$$

where T is the section thickness, a_i is the area of orbital cavity in section i that is manually selected, and m is the total number of slices containing the region of interest.

Stereological technique

Stereological orbital volume measurements were performed using the Analyze software (Mayo Foundation, Rochester, MN, USA). Stereology is a mathematical approach for estimating geometrical quantities and volume. It is based on Cavalieri's principle, which involves systematic random sampling through the region of interest. Instead of tracing the region, sampling points over the region of interest are marked. Every point has a given area associated with it. The area of the organ of interest in a given section is the number of points selected times their associated area. That result is multiplied by the thickness and the interval of the sections to estimate a given volume. In our image dataset a square systematic array of test points was overlayed in each cross-section. Thereafter, all points lying within the area of the orbital cavity are selected by the user and the software automatically calculates the total number of point counts (Fig. 2c). The grid was randomly placed in the initial image and its orientation was kept constant for all the subsequent images. The total volume (V) was given by Eq. 2:

$$V = TA \sum_{i}^{m} P_i$$

where T is the distance between two consecutive sections used for stereological estimations, A is the area of each test point, m is the number of the sections depicting the orbit and P_i is the number of points lying within the orbital cavity on section i.

The precision of stereological object volume estimation may be determined by its coefficient of error (CE) as reported by Gundersen and Jensen [19]. The Analyze software automatically provided the CE related to each orbital volume assessment.

CE is dependent upon the separation distance between the test points of the grid. The point spacing of the grid may be given by Eq. 4:

$$d = \sqrt{\frac{V}{N \cdot T}}$$

where V is an approximation of the volume of interest, N is the total number of counted points and T is the interval

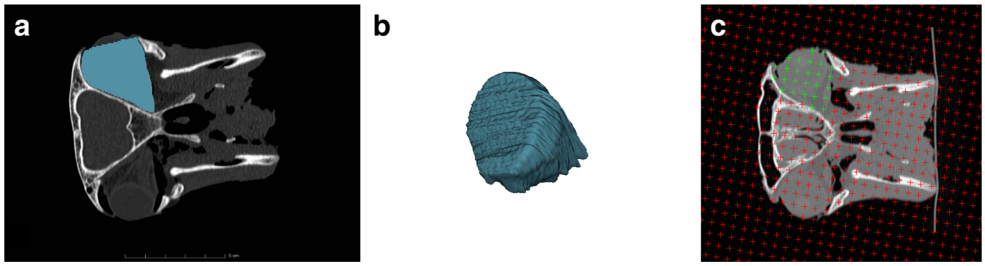

Fig. 2 **a** Manual delineation of the orbital boundaries in axial slices using 3D volume rendering in 3D Slicer. **b** 3D-model of the segmented orbit for measuring its total volume. **c** Stereological approach of the orbital volume using the Analyze software. The green points within the area of the orbital cavity were selected by the user and the total volume is estimated automatically based on the total number of point counts

between two consecutive sections used for stereological estimations.

It is recommended that about 100–200 point counts may provide efficient stereological estimations [17]. Therefore, volume estimations were also performed by selecting 150 test points in all sections. The distance d in Eq. 4 was found by using an N equal to 150 points.

Stereology sampling and optimization

The stereological method enables the assessment of any organ volume together with its CE by using only a sample of slices containing the organ of interest. Previous studies have indicated the efficiency of systematic slice sampling for volumetric analysis [20, 21]. This optimal approach should involve the minimum number of systematically sampled slices required to provide acceptable volume assessments with the minimum user intervention. Gundersen and Jensen [19] reported that a CE of 5% is sufficient in stereological studies. To optimize the stereological technique, we randomly selected the right orbit of the third skull and we performed several estimations. We used sampling intensities of 1/2, 1/3, 1/4, 1/5, 1/6, 1/8, 1/10 and 1/12. For instance, the orbit of the third skull was depicted in 59 slices. The sample type of 1/5 could provide the five different systematic samples: {1,6,11,16,21,26,31,36,41,46,51,56}, {2 , 7 , 1 2 , 1 7 , 2 2 , 2 7 , 3 2 , 3 7 , 4 2 , 4 7 , 5 2 , 5 7}, {3 , 8 , 1 3 , 1 8 , 2 3 , 2 8 , 3 3 , 3 8 , 4 3 , 4 8 , 5 3 , 5 8}, {4 , 9 , 1 4 , 1 9 , 2 4 , 2 9 , 3 4 , 3 9 , 4 4 , 4 9 , 5 4 , 5 9}, {5,10,15,20,25,30,35,40,45,50,55}. One of these samples was randomly chosen for orbital volume estimation. The optimization procedure aimed to define the proper point spacing that would provide acceptable volume estimations using the minimum number of systematically sampled CT sections.

Imaging in human subjects

The same imaging protocol was used to obtain CT image datasets in five human subjects. Post-processing analysis included orbital segmentation and quantification using planimetry and stereology as described above (Fig. 3). CE of error was also reported to evaluate the performance of stereology in human orbits.

Statistical analysis

Statistical analysis was performed using SPSS (IBM SPSS Statistics for Windows, Version 22.0). Descriptive statistics are presented as mean ± SD. All *p*-values relate to two-sided tests with a significance level of a = 0.05. A non-parametric Mann-Whitney test was used to detect differences between groups.

To test the proportion of agreement among measurements, we tested intra-observer and inter-observer agreement as follows:

Intra-observer reliability of CT measurements was calculated by comparing two separate

measurements performed by one observer 1 month apart to minimize recall bias.

Inter-observer reliability of CT measurements was calculated by comparing volume measurements of two separate observers, using the same methodology. The intraclass correlation coefficient (ICC) (two-way mixed model) was computed to estimate the inter-rater and intra-rater reliability. An ICC value of > 0.7 in absolute single measures was considered to be acceptable agreement.

To compare the volumetric techniques, Pearson's correlation coefficient was used to find significant correlations between data from planimetry stereology and water displacement techniques. Furthermore, a paired samples *t*-test was applied to identify significant differences in the mean values of the computed volumes.

In addition, the Bland-Altman statistical test was used to determine 95% limits of agreement between the stereological and the planimetric technique. The 95% limits of agreement were defined as the mean difference ± 1.96 SD, where SD is the standard deviation of the differences. In all statistical analyses *p*-values less than 0.05 were considered as statistically significant

Graphic displays were illustrated using GraphPad Prism (Graphpad Software Inc, La Jolla, CA, USA).

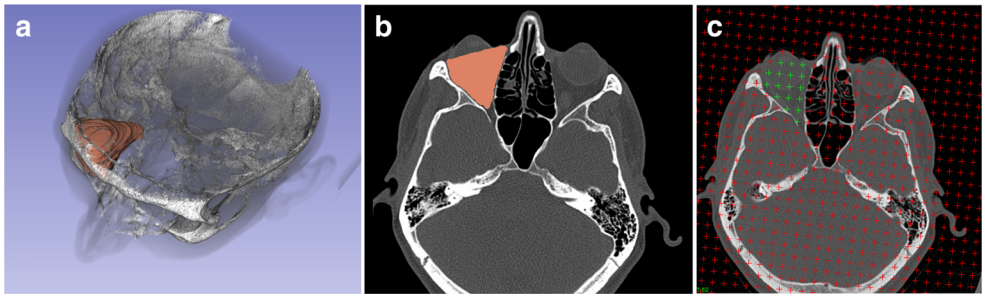

Fig. 3 **a** Model of the segmented orbit within the human skull, using 3D slicer. **b** Manual delineation of the human orbit. Using planimetry, the selected areas are added and then multiplied by slice thick to measure the total volume. **c** Stereological method, using 1/8 sampling, for calculating the orbital volume by selecting points that lie in the orbital cavity

Results

For this analysis, five models (10 orbits in total) were considered. Typically, 60 CT slices were needed to cover the entire sheep's orbit. The volumes measured by the water displacement technique ranged between 16.82 cm^3 and 18.59 cm^3, while the mean orbital volume measured was 17.81 ± 0.59 cm^3 (Tables 2 and 3).

Definition of the optimal stereological approach

The precision of the obtained stereological orbital volume estimations is presented in Table 1. The CE exceeded the target precision of 5% when systematic sampling intensities of 1/10 and 1/12 were adopted. Volume assessments on the entire slice set depicting an orbital cavity resulted in a CE of 0.38%. The corresponding CE with the use of a sample consisting of every sixth or eighth CT slice was 1.89% and 2.59 ± 1.0%, respectively (Table 1). The mean time for volumetry using a sample of slices generated from a systematic sampling intensity of 1/6 and 1/8 depicting the orbit was 2.3 min and 1.9 min, respectively. When compared with the actual volume of the water-filling measurements, the 1/6 and 1/8 sampling results displayed a percent difference of 5.41% and 4.57%, respectively. Based on the above data, the application of stereology on a sample of slices arising from the 1/8 systematic sampling scheme was considered as the optimal and time efficient approach. This approach could provide quick volume estimates with an acceptable level of precision. The 1/8 sampling was used for stereological estimation in the animal and human orbits.

Image volumetry in animal models

Using *planimetry* (Table 2), the first investigator reported a mean orbital volume of 17.87 ± 0.68 cm^3 in the first and 17.93 ± 0.66 cm^3 in the second evaluation, which was not significantly different ($p = 0.853$, Mann-Whitney test). Furthermore, the ICC showed high intra-rater agreement (ICC=0.993, $p \approx 0.001$). Additionally, the second investigator measured a mean orbital volume of 17.93 ± 0.48 cm^3, which was also not statistically significant compared with the first evaluation of the first investigator ($p = 0.850$, Mann-Whitney test), and displayed an excellent inter-rater agreement (ICC=0.990; $p \approx 0.001$). The average measurement time for each data set was 18.6 min.

Using *stereology* sampling of 1/8 (Table 3) as described above, the first investigator reported a mean

Table 1 Stereological orbital optimization: Model 3 – right orbit

Sample Type	Number of Measured slices	Sectioning Thickness (T) (mm)	Separation distance d (mm) for 150 points	Measured Volume (cm^3)	CE (%)	Measurement Time (min)
1/1	60	0.625	14.6	18.55	0.38	8.2
1/2	30	1.25	10.3	18.16	0.61	5.5
1/3	20	1.875	8.4	17.73	0.77	3.9
1/4	15	2.5	7.3	17.60	1.15	3.1
1/5	12	3.125	6.5	18.07	1.74	2.7
1/6	10	3.75	6	17.61	1.89	2.3
1/8	8	5	5.2	17.76	2.59	1.9
1/10	6	6.25	4.6	15.24	5.15	1.6
1/12	5	7.5	4.2	18.38	7.32	1.2

Table 2 Orbital volume planimetry measurements

Orbital Cavity	Investigator 1 First measurement (cm^3)	Investigator 1 Second measurement (cm^3)	Investigator 2 Measurement (cm^3)	Mean value in planimetry (cm^3)	Intrapersonal difference (cm^3)	Interpersonal difference (cm^3)	Water displacement (gold standard)
Model 1							
Left orbit	18.31	18.43	18.39	18.38	0.12	0.06	18.12
Right orbit	17.87	17.91	17.94	17.91	0.04	0.05	17.86
Model 2							
Left orbit	17.64	17.61	17.72	17.66	0.03	0.09	17.53
Right orbit	17.85	17.99	17.87	17.90	0.14	0.05	17.74
Model 3							
Left orbit	18.49	18.57	18.44	18.50	0.08	0.09	18.45
Right orbit	18.75	18.82	18.88	18.82	0.07	0.11	18.59
Model 4							
Left orbit	18.28	18.20	18.27	18.25	0.08	0.03	18.13
Right orbit	18.11	18.09	18.17	18.12	0.02	0.07	18.04
Model 5							
Left orbit	16.60	16.78	16.85	16.74	0.18	0.16	16.82
Right orbit	16.87	16.92	16.77	16.85	0.05	0.13	16.90

orbital volume of 17.54 ± 0.49 cm^3 (CE= 2.81± 0.15%) in the first and 17.57 ± 0.48 cm^3 (CE= 2.68 ± 0.21%) in the second evaluation, which was not significantly different (p = 0.739, Mann-Whitney test). Furthermore, the ICC showed an excellent intra-rater agreement (ICC=0.995; $p \approx 0.001$). Additionally, the second investigator reported a mean orbital volume of 17.56 ± 0.47 cm^3 (CE= 2.51± 0.11%) in his assessment, which was also not statistically significant compared with the first evaluation of the first investigator (p = 0.912, Mann-Whitney test), and a high inter-rater agreement was found in ICC (ICC=0.990; $p \approx 0.001$)

To compare the different methods, we correlated the data from the first measurement of the first investigator with the water-filling method. The measured data from planimetry, stereology and water displacement methods followed a normal distribution as confirmed by the Kolmogorov-Smirnov test (p = 0.2, p = 0.161 and p = 0.2, respectively).

Table 3 Orbital volume stereology measurements

Orbital Cavity	Investigator 1 First measurement (cm^3)	Investigator 1 Second measurement (cm^3)	Investigator 2 Measurement (cm^3)	Mean value in stereology (cm^3)	Intrapersonal difference (cm^3)	Interpersonal difference (cm^3)	Water displacement (gold standard)
Model 1							
Left orbit	17.93	17.97	17.99	17.96	0.04	0.04	18.12
Right orbit	17.88	17.89	17.91	17.89	0.01	0.02	17.86
Model 2							
Left orbit	17.41	17.45	17.36	17.41	0.04	0.07	17.53
Right orbit	17.62	17.57	17.59	17.59	0.05	0.01	17.74
Model 3							
Left orbit	17.71	17.73	17.65	17.70	0.02	0.07	18.45
Right orbit	17.76	17.83	17.88	17.82	0.07	0.08	18.59
Model 4							
Left orbit	17.90	17.90	17.92	17.91	0.00	0.02	18.13
Right orbit	17.89	17.95	17.85	17.90	0.06	0.07	18.04
Model 5							
Left orbit	16.53	16.64	16.67	16.61	0.11	0.08	16.82
Right orbit	16.82	16.77	16.81	16.80	0.05	0.09	16.90

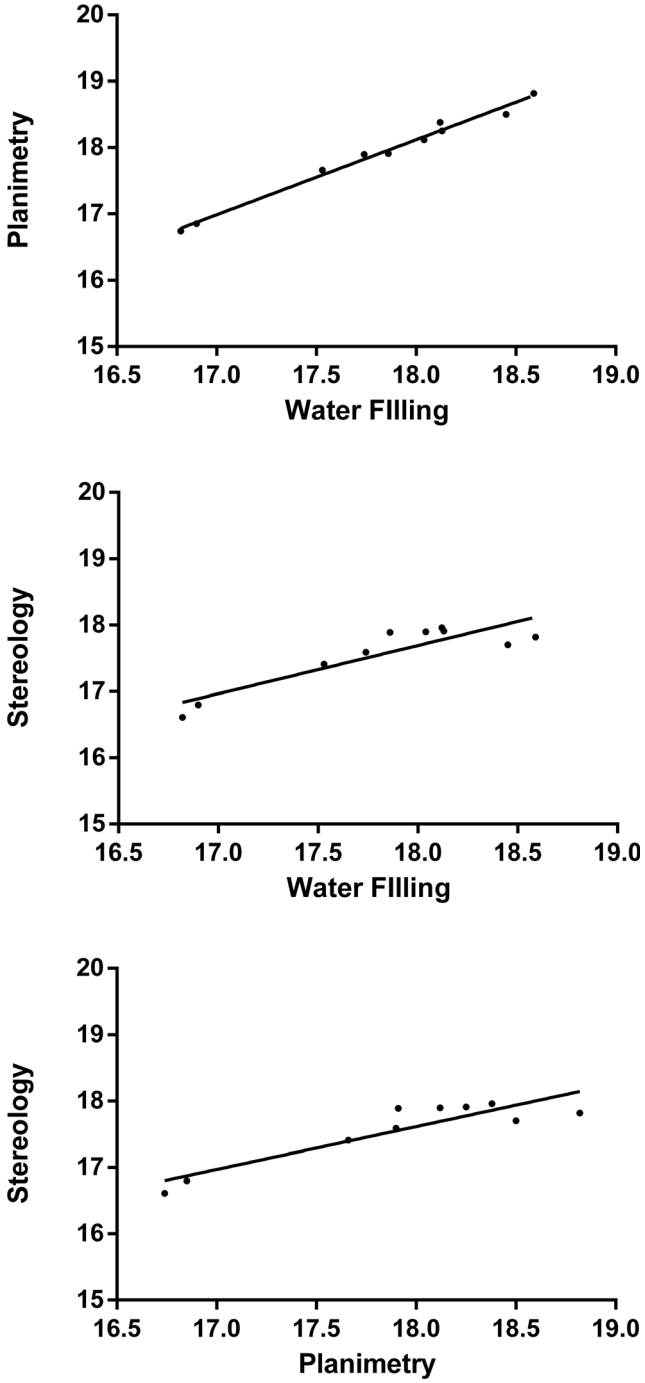

Fig. 4 Correlations between the total volumes obtained by planimetry, stereology and water-filling methods

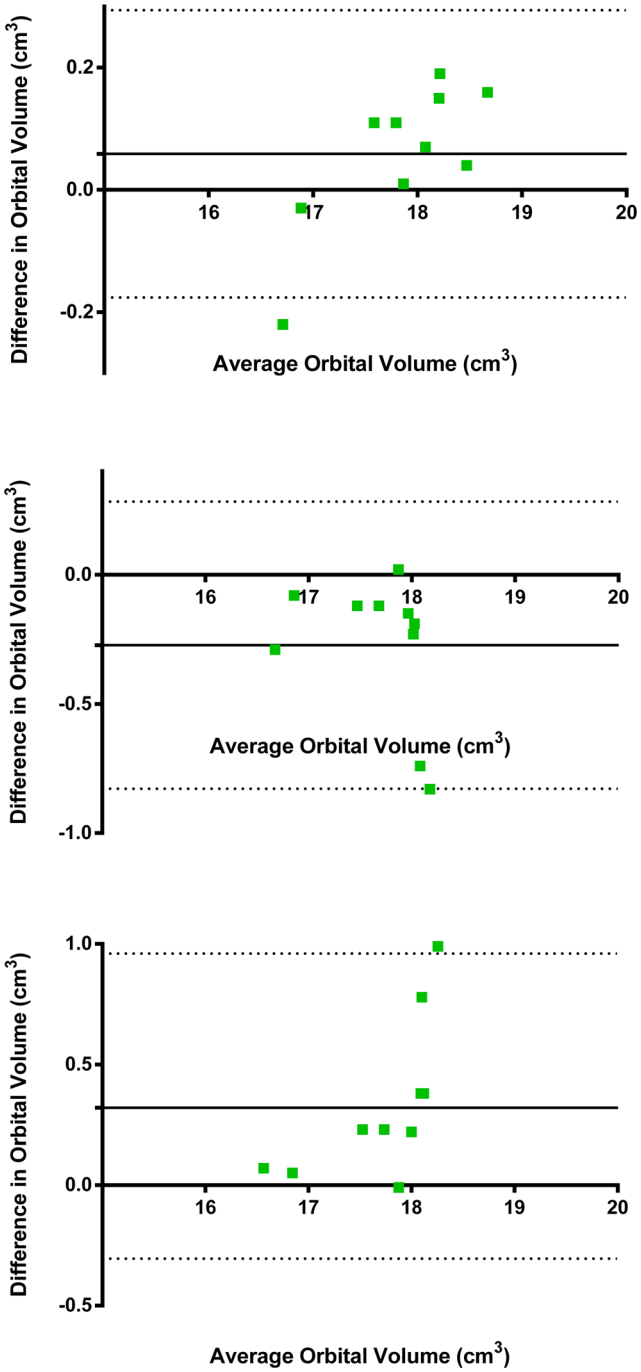

Fig. 5 Upper plot: differences in orbital volume estimates as defined by manual planimetry and the water-filling method. The mean difference is presented with the solid line whereas the 95% limits of agreement are shown with the dotted lines. Middle plot: differences in orbital volume estimates as defined by the optimized stereological approach and the water-filling method. Lower plot: differences in orbital volume measurement as defined by manual planimetry and stereology

Total volumes obtained by stereology were highly correlated with the water-filling method (r=0.893; p = 0.001) while paired samples t-test yielded a statistically significant difference between the mean volumes computed by the water-filling method and stereology (t=3.047; p = 0.014). In addition, planimetry results also displayed high correlation with the water-filling method (r=0.957; $p \approx 0.001$) but a paired samples t-test did not reveal a significant difference (p = 0.154). Finally, between planimetry and stereology a strong correlation was also noted (r=0.909; $p \approx 0.001$) and a paired t-test displayed a statistically significant difference in mean values (t=3.254; p = 0.01) (Fig. 4).

The exact limits of agreement between the planimetry and water filling as well as between the stereology and water-filling methods are presented in the Bland-Altman scatter plots shown in Fig. 5. The mean difference of the orbital volume using the planimetry and the water-filling techniques was 0.059 cm^3. The SD of the differences was 0.119 cm^3. Therefore, the limits of agreement were equal to -0.176 and 0.294 cm^3. All but one data point were between the above limits of agreement (Fig. 5). The mean difference of the orbital volume using stereology and water-filling methods was -0.273 cm^3. The SD of the differences was 0.283 cm^3. Therefore, the limits of agreement were equal to -0.823 and 0.283 cm^3. All, apart from one, data points were between the above limits of agreement (Fig. 5). Finally, the mean difference of the orbital volume using planimetry and stereology was 0.332 cm^3. The SD of the difference was 0.322 cm^3 and the limits of agreement were noted at -0.301 cm^3 and 0.964 cm^3.

Image volumetry in human subjects

The same methodologies of planimetry and stereology were used to estimate the volumetry of five healthy subjects (10 total orbits). The measured volumes by planimetry (Fig. 3b) ranged between 18.74 cm^3 and 19.63 cm^3, while the mean orbital volume was 19.11 ± 0.49 cm^3. Using stereology sampling of 1/8 (Fig. 3c), the estimated volume ranged between 18.57 cm^3 and 19.27 cm^3, and the mean orbital volume was found to be 19.05 ± 0.50 cm^3 with a CE of 3.75 ± 0.16 % (Table 4). The mean measure time was 2.1 ± 0.1 min. Total volumes obtained by planimetry were highly correlated with the those obtained from stereology (r=0.909; $p \approx 0.001$, Pearson's correlation coefficient).

Discussion

Our study suggests that both planimetry and stereology methods can be applied in a given orbital area for precise measurements. In fact, both techniques displayed significant correlation with the direct water-filling measurements, r=0.957 for planimetry and r=0.893 for stereology. In this analysis we evaluated the applicability of planimetry and stereology in measuring the orbital volume in both sheep craniums and humans. We optimized stereological volume measurements through a systemic sampling process and we defined the minimum number of CT slices required to provide acceptable orbital volume estimates. Our findings suggest that 1/8 stereological sampling can be used for both animal and human subjects by minimizing the required time for measurements to about 1.9 min. Finally, we evaluated the comparative performance of stereology against manual planimetry. The two methods yielded a strong correlation (r=0.909). Bland-Altman analysis indicated that stereology tends to slightly underestimate the actual volume of a given orbit by a small amount (mean difference in volume= 0.273 cm^3)

Our results are important for guiding clinical decisions since several physiological and pathological conditions may contribute to changes in the orbital volume [22], for example, exophthalmos, as seen in Graves' disease, and enophthalmos, which is a common condition after trauma and orbital fractures. Small changes in volume can lead to severe change in the axial position of the eye. It has been estimated that a 1 cm^2 increase in orbital volume will result in 1 mm of axial displacement of the globe [4]. Thus, determination of the orbital volume is essential when studying the pathobiology of Graves' orbitopathy or craniofacial syndromes (e.g. Apert's syndrome), or for surgical planning of orbital decompression

Table 4 Orbital volumetry in human subjects

Orbital Cavity	Volume measured by planimetry (cm^3)	Volume measured by stereology (cm^3)	Stereology CE (%)
Subject 1			
Left orbit	18.74	18.91	3.97
Right orbit	18.66	18.78	3.14
Subject 2			
Left orbit	19.63	19.86	3.37
Right orbit	20.15	19.97	4.10
Subject 3			
Left orbit	18.75	18.73	2.92
Right orbit	18.81	18.63	3.57
Subject 4			
Left orbit	19.12	19.27	3.92
Right orbit	19.54	19.13	4.34
Subject 5			
Left orbit	18.92	18.69	4.53
Right orbit	18.77	18.57	3.66

and reconstruction. In cases of enophthalmos, decision making and surgical planning is based on the severity of injury. However, the amount of globe intrusion is often masked by periorbital swelling and management is usually delayed until swelling resolves. But if surgery is carried out at a later stage, treatment of enophthalmos becomes more difficult because of the muscular atrophy and fibrosis of the periorbital soft tissue [23]. Unfortunately, in clinical practice, orbital volume changes are often evaluated in a qualitative and subjective mode, rather than a quantitative and objective fashion. Surgical results also lack quantification. The reason for this inadequate management is that most volumetric procedures are time consuming, require manual work from trained staff and, therefore, are poorly applicable in clinical practice. Several stereological volume measurements in different organs have been studied using MRI and CT [24–26]. However, to the best of our knowledge, this is the first study employing an *ex vivo* methodology and objectively testing the validity of findings of both planimetry and stereology on CT datasets, as opposed to previous cadaver studies [15, 27].

A limitation of this study is that it does not consider the significant variability of orbital volume in the healthy population. These changes account for anatomical variations, race and gender [22]. A larger pool of patients should be tested taking into account the epidemiological discrepancies of the studied structures. Moreover, our proposed methods were not tested in a pediatric population where the orbital socket is considered more complex in terms of anatomical relationships and image segmentation. Another limitation to be considered in clinical practice is that the semi-automated methodology we described requires user training and cannot be implemented without the appropriate software. An operational system using a fully automated algorithm needs to be designed for future testing. For the presented study, a slice thickness of 0.625 mm was used. Finally, we used imaging data obtained solely from CT scans. Further research is required to examine the validity of stereological measurements on CT and MRI scans acquired with different slice thicknesses from that used in the current work.

In this study, we tried to evaluate the applicability of planimetry and stereology in orbital volume evaluation, using CT imaging, with a view to eliminating subjective bias. Stereological measurements were comparable to manual planimetry, which is a strong indicator about the accuracy of our method. Apart from providing reliable and precise estimations of the orbital volume, they are advantageous as a rather objective and time-efficient method. Application can be extended in basic research on orbital measurements, in ophthalmic pathology, surgical planning and quality control following orbital reconstructions.

Funding This study has received funding by the General Secretariat for Research and Technology (GSRT) and the Hellenic Foundation for Research and Innovation (HFRI).

Compliance with ethical standards

Guarantor The scientific guarantor of this publication is Efstathios Detorakis.

Conflict of interest The authors of this manuscript declare no relationships with any companies whose products or services may be related to the subject matter of the article.

Statistics and biometry One of the authors has significant statistical expertise.

Informed consent Written informed consent was obtained from all subjects (patients) in this study.

Ethical approval Institutional Review Board approval was obtained.

Methodology
- Prospective
- Experimental
- Performed at one institution

References

1. Alinasab B, Beckman MO, Pansell T, Abdi S, Westermark AH, Stjärne P (2011) Relative difference in orbital volume as an indication for surgical reconstruction in isolated orbital floor fractures. Craniomaxillofac Trauma Reconstr. 4:203–212
2. Imai K, Fujimoto T, Takahashi M, Maruyama Y, Yamaguchi K (2013) Preoperative andpostoperative orbital volume in patients with Crouzon and Apert syndrome. J Craniofac Surg 24:191–194
3. Schiff BA, McMullen CP, Farinhas J et al (2015) Use of computed tomography to assess volume change after endoscopic orbital decompression for Graves' ophthalmopathy. Am J Otolaryngol 36: 729–735
4. Sung YS, Chung CM, Hong IP (2013) The correlation between the degree of enophthalmos and the extent of fracture in medial orbital wall fracture left untreated for over six months: a retrospective analysis of 81 cases at a single institution. Arch Plast Surg. 40: 335–340
5. Oh TS, Jeong WS, Chang TJ, Koh KS, Choi JW (2016) Customized orbital wall reconstruction using three-dimensionally printed rapid prototype model in patients with orbital wall fracture. J Craniofac Surg. 27:2020–2024
6. Forbes G, Gorman CA, Gehring D, Baker HL Jr (1983) Computer analysis of orbital fat and muscle volumes in Graves ophthalmopathy. AJNR Am J Neuroradiol. 4:737–740
7. Forbes G, Gehring DG, Gorman CA, Brennan MD, Jackson IT (1985) Volume measurements of normal orbital structures by computed tomographic analysis. AJR Am J Roentgenol. 145:149–154
8. McGurk M, Whitehouse RW, Taylor PM, Swinson B (1992) Orbital volume measured by a low-dose CT scanning technique. Dentomaxillofac Radiol. 21:70–72
9. Lutzemberger L, Salvetti O (1998) Volumetric analysis of CT orbital images. Med Biol Eng Comput. 36661-666
10. Deveci M, Oztürk S, Sengezer M, Pabuşcu Y (2000) Measurement of orbital volume by a 3-dimensional software program: an experimental study. J Oral Maxillofac Surg. 58:645–648
11. Warfield SK, Kaus M, Jolesz FA, Kikinis R (2000) Adaptive, template moderated, spatially varying statistical classification. Med Image Anal. 4:43–55

12. Bartling SH, Majdani O, Gupta R et al (2007) Large scan field, high spatial resolution flat-panel detector based volumetric CT of the whole human skull base and for maxillofacial imaging. Dentomaxillofac Radiol. 36:317–327
13. Bijlsma WR, Mourits MP (2006) Radiologic measurement of extraocular muscle volumes in patients with Graves' orbitopathy: a review and guideline. Orbit. 25:83–91
14. Cooper WC (1985) A method for volume determination of the orbit and its contents by high resolution axial tomography and quantitative digital image analysis. Trans Am Ophthalmol Soc. 83:546–609
15. Acer N, Sahin B, Ergür H, Basaloglu H, Ceri NG (2009) Stereological estimation of the orbital volume: a criterion standard study. J Craniofac Surg. 20:921–925
16. Mazonakis M, Karampekios S, Damilakis J, Voloudaki A, Gourtsoyiannis N (2004) Stereological estimation of total intracranial volume on CT images. Eur Radiol. 14:1285–1290
17. Unal B, Kara A, Aksak S, Unal D (2010) A stereological assessment method for estimating the surface area of cycloids. Eurasian J Med 42:66–73
18. Bilgic S, Sahin B, Sonmez OF et al (2005) A new approach for the estimation of intervertebral disc volume using the Cavalieri principle and computed tomography images. Clin Neurol Neurosurg 107: 282–288
19. Gundersen HJ, Jensen EB (1987) The efficiency of systematic sampling in stereology and its prediction. J Microsc. 147:229–263
20. Roberts N, Puddephat MJ, McNulty V (2000) The benefit of stereology for quantitative radiology. Br J Radiol. 73:679–697
21. Mazonakis M, Damilakis J, Varveris H (1998) Bladder and rectum volume estimations using CT and stereology. Comput Med Imaging Graph. 22:195–201
22. Furuta M (2001) Measurement of orbital volume by computed tomography: especially on the growth of the orbit. Jpn J Ophthalmol. 45:600–606
23. Sugamata A, Yoshizawa N (2010) Clinical analysis of orbital blowout fractures caused by a globe-to-wall contact mechanism. J Plast Surg Hand Surg. 44:278–281
24. Sahin B, Emirzeoglu M, Uzun A et al (2003) Unbiased estimation of the liver volume by the Cavalieri principle using magnetic resonance images. Eur J Radiol. 47:164–170
25. Mazonakis M, Pagonidis K, Damilakis J (2011) Right ventricular volumes and ejection fraction by MR imaging and stereology: comparison with standard image analysis method. Clin Anat. 24:868–873
26. Mazonakis M, Stratakis J, Damilakis J (2015) Efficient stereological approaches for the volumetry of a normal or enlarged spleen from MDCT images. Eur Radiol. 25:1761–1767
27. Emirzeoglu M, Sahin B, Selcuk MB, Kaplan S (2005) The effects of section thickness on the estimation of liver volume by the Cavalieri principle using computed tomography images. Eur J Radiol. 56:391–397